Available online at www.sciencedirect.com
ScienceDirect
Journal of Organometallic Chemistry 692 (2007) 4969–4977
Journal of Organometallic Chemistry
www.elsevier.com/locate/jorganchem

Metal induced enhancement of fluorescence and modulation of two-photon absorption cross-section with a donor–acceptor–acceptor–donor receptor

Sanjib Das, Amit Nag, Kalyan K. Sadhu, Debabrata Goswami, Parimal K. Bharadwaj *

Department of Chemistry, Indian Institute of Technology, Kanpur 208 016, India

Received 17 May 2007; received in revised form 12 July 2007; accepted 13 July 2007
Available online 19 July 2007

Abstract

A metal ion sensing fluorophore **L** that exhibits a large two-photon absorption cross-section has been synthesized in good yields. The influences of different metal ion inputs, on the one- and two-photon spectroscopic properties of **L**, have been investigated. The ligand itself does not show any fluorescence although in presence of a metal ion like Zn(II), Cd(II), Mg(II) or Ca(II), a ~25 time enhancement of fluorescence is observed. The ligand with symmetrical "donor–acceptor–acceptor–donor" characteristics exhibits a large two-photon absorption cross-section measured by femtosecond open-aperture Z-scan technique at 880 nm. However, presence of any of the above metal ions lowers its two-photon absorption cross-section (δ) to different extents at 880 nm. Theoretical calculation carried out in DFT formalism on the ligand and its Zn(II) complex corroborate experimental results.

Keywords: Metal ion receptor; OPA; TPA; Fluorescence; DFT

1. Introduction

The prospect of developing new materials exhibiting third-order NLO property measured in terms of two-photon absorption cross-section (δ) has received increasing attention in recent years, due to their potential applications [1] in opto-electronics and photonic devices. These molecules are of relevance in the emerging areas of two-photon laser scanning microscopy (TPLSM) [1a], optical power limiting [1b], three-dimensional (3D) optical data storage [1c], two-photon up-conversion lasing [1d], photodynamic cancer therapy [1e], and so on. Particularly, fluorescence active molecules with large two-photon absorption cross-section δ (i.e., $\delta > 1000$ GM; $1\ \mathrm{GM} = 1 \times 10^{-50}\ \mathrm{cm^4\ s\ photon^{-1}\ molecule^{-1}}$) with the excitation wavelength well removed from the range, 600–1300 nm are important in TPLSM applications. However, well-defined molecular structure–property relationships for third order nonlinear optical chromophores and TPA activity are still absent. However, search for molecular guidelines to have large TPA cross-section (δ) has led to molecules with asymmetric donor–π-bridge–acceptor (D–π–A) and symmetric donor–π-bridge–donor (D–π–D), acceptor–π-bridge–donor–π-bridge–acceptor (A–π-D–π–A), and donor–π-bridge–acceptor–π-bridge–donor (D–π–A-π–D) conjugated structural motifs. Both theoretical considerations and experimental results lead to the molecules with high TPA activity as the ones where donor and acceptor groups are symmetrically disposed resulting in a substantial symmetric intramolecular charge re-distribution upon excitation [2]. These studies also reveal that the effect of molecular charge transfer symmetry, donor/acceptor group strength, chromophore number density and length of the conjugated π backbone are the most important factors affecting the molecular TPA activity [3]. So far, the TPA phenomenon has focused mostly on organic dipolar [4] and less on quadrupolar [5], octupolar [6], and dendritic

* Corresponding author. Tel.: +91 512 259 7034; fax: +91 512 259 7436.
E-mail address: pkb@iitk.ac.in (P.K. Bharadwaj).

0022-328X/$ - see front matter © 2007 Elsevier B.V. All rights reserved.
doi:10.1016/j.jorganchem.2007.07.013

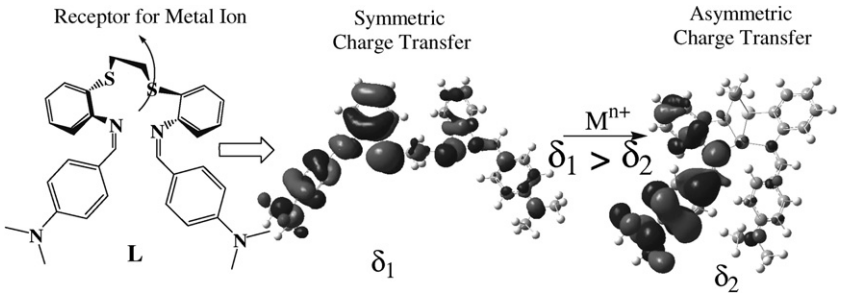

Scheme 1. Plan for modulation of TPA response in a D–π–D′ type receptor system. D, donor; π, ethylenic conjugated moieties; M^{n+}, Zn(II), Cd(II), Mg(II) and Ca(II) ions.

[7] molecules and to very few extents with metal complexes [8]. Very recently, we have shown that simple metal ion recognition events lead exceptionally large values of TPA cross-sections known for any coordination metal complexes in a weakly polarized conjugated Schiff base ligand [9].

Further, it is important to develop systems that not only show high δ values but also have the ability to respond the presence of various ionic/neutral analytes through modulation of their TPA responses. Few synthetic approaches [10] and theoretical calculations are reported [10,11] in the literature on ways to modulate molecular TPA properties. Jiang et al. has synthesized different stilbene based symmetrically (D–π–D) and asymmetrically (D–π–A) substituted conjugated dipolar chromophores [10] and showed a comparative study of the TPA activity for symmetrically and asymmetrically substituted chromophores. The TPA efficiency decreases on going from D–π–D to D–π–A molecules. Theoretical calculations carried out by this group for symmetrically and asymmetrically substituted chromophores point to the fact that the transition dipole moment (M_{ee} or $M_{ee'}$) function is the most important factor in modulating the molecular TPA efficiency, which is very high for symmetrically substituted stilbene chromophores in comparison to asymmetrically substituted chromophores. Relevance of transition dipole moment in predicting TPA efficiency was originally put forth by Marder and coworkers [2]. However, majority of regular dipolar compounds show δ values that typically do not exceed 10–300 GM ($1\ \mathrm{GM} = 10^{-50}\ \mathrm{cm^4\ s\ photon^{-1}\ molecule^{-1}}$) measured by femtosecond laser.

Metal ions are excellent 3D template and can assemble simple organic NLO-phores around with concomitant tuning of the molecular nonlinear optical property by virtue of inducing a strong intra-ligand charge-transfer (ILCT) as well as low-energy metal–ligand charge transfer (MLCT) transitions. Herein, we report a new highly TPA active acyclic receptor (**L**), synthesized by Schiff base condensation of 4-(dimethylamino)benzaldehyde with 1,2-di(*o*-aminophenolthio)ethane. The ligand **L** is a D–π–π′–π–D analogue since the imine part possesses less electron-donating character with respect to the dimethylamine moiety and instead of having a small-saturated carbon chain in the thioether part (π′, as obtained in HOMO of ligand) the π conjugation is affected a lot. Binding of metal ions such as Zn(II), Cd(II), Mg(II) or Ca(II) to the imine N as well as sulfur atoms of **L** renders them as acceptors i.e. D–π–π′–π–D changes to a D–π–σ–π–D analogue with reduction of TPA activity (Scheme 1) where the binding of metal ion with thio ether moiety plays the crucial role by snapping the conjugation. Interestingly, the ligand does not show any significant fluorescence but on complexation with any of the above mentioned metal ions, exhibits ~25-fold enhancement of fluorescence. Although enhancement is not very large, it provides a starting point for ligand design.

The metal ions probed in this study are biologically important. Many enzymatic reactions are mediated by Mg(II) ions whereas Ca(II) ion acts as an universal second messenger in cells [12]. Few studies have been reported [13] in the literature on the TPA properties of chromophores that respond to different ions such as calcium orange, calcium green-I, and calcium crimson with δ values in the range of 1–30 GM in the unbound state. Upon binding of calcium ions, δ values increase to 50–100 GM. On the other hand, Mg(II) was shown to lower the δ values by 50% while showing fluorescence enhancement in an aza-crown ether connected to distyrylbenzenes in the D–π–A–π–D format [14].

2. Experimental

2.1. Materials

Reagent grade 4-(dimethylamino)benzaldehyde, 1-fluoro-2-nitrobenzene, palladium on carbon 5%, Rhodamine-6G, 1,2-ethanedithiol and perchlorate salts of different metals used in the study were acquired from Aldrich and used as received. Reagent grade hydrazine hydrate, K_2CO_3 and all the solvents were received from S.D Fine Chemicals, India. All solvents were freshly distilled prior to use.

2.2. Synthesis of *L*

The synthetic route adopted for **L** is given in Scheme 2.

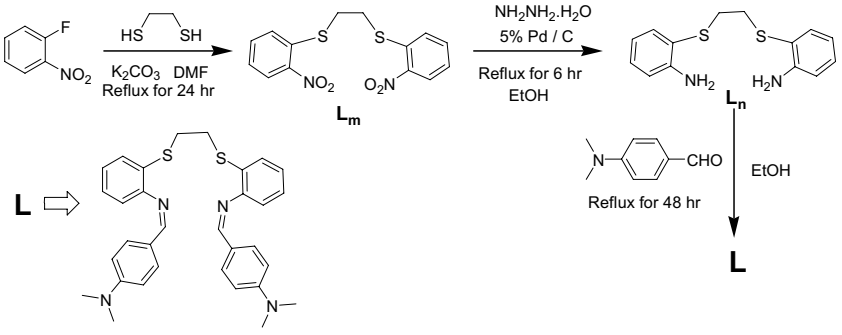

Scheme 2. Synthetic route for D–π–D′ type highly TPA active cationic receptor.

*2.2.1. 1,2-Di(o-nitrophenolthio)ethane (**L**$_m$)*

To a solution of 1,2-ethanedithiol (0.94 g, 1 mmol) in dry DMF (10 mL) was added anhydrous K_2CO_3 (0.35 g, 2.5 mmol) and the reaction mixture was stirred for 1 h. subsequently, a solution of 1-fluoro-2-nitrobenzene (0.31 g, 2.2 mmol) in DMF (10 mL) was added dropwise for 15 min and the reaction mixture was stirred for 24 h at RT. The reaction mixture is further heated at 70 °C for 15 h to complete the reaction. After cooling to RT, the reaction mixture was poured into ice-cold water (100 mL). The light yellow solid separated was collected by filtration and washed repeatedly with water (5 × 100 mL). Yield ~90%; m.p. 175 °C; ^{1}H NMR: δ 2.87 (s, 4H), 7.52–7.41 (m, 8H); ES-MS (*m*/*z*): 335(50%) $[M-H]^+$. Anal. Calc. for $C_{14}H_{12}N_2O_4S_2$: C, 49.99; H, 3.60; N, 8.33. Found: C, 50.08; H, 3.69; N, 8.43%.

*2.2.2. 1,2-Di(o-aminophenolthio)ethane (**L**$_n$)*

In a two-necked round-bottomed flask equipped with a reflux condenser and a dropping funnel was prepared a suspension of dinitro compound $\mathbf{L_m}$ (0.33 g, 1 mmol), palladium on carbon 5% (0.05 g), and absolute ethanol (15 mL). The mixture was warmed with stirring and subsequently hydrazine hydrate 80% (3 mL) in ethanol (10 mL) was added dropwise over a 1 h period through the dropping funnel with temperature maintained at about 50 °C. The reaction mixture was refluxed for 6 h and filtered while hot. On cooling, the filtrate gave the corresponding diamino compound $\mathbf{L_n}$ as a white solid after vacuum drying. Yield ~95%; m.p. 154 °C; ^{1}H NMR: δ 2.82 (s, 4H), 7.42–7.35 (m, 8H); ES-MS (*m*/*z*): 275 (60%) $[M-H]^+$. Anal. Calc. for $C_{14}H_{16}N_2S_2$: C, 60.83; H, 5.83; N, 10.13. Found: C, 60.89; H, 5.87; N, 10.21%.

*2.2.3. Synthesis of **L***

A mixture of 4-(dimethylamino)benzaldehyde (0.37 g, 2.5 mmol) and $\mathbf{L_n}$ (0.28 g, 1 mmol) were dissolved in 10 mL absolute ethanol and heated in an oil bath at 80 °C with stirring for 48 h in the dark. Cooling the reaction mixture at room temperature afforded a yellow solid. The yellow solid was collected by filtration, washed thoroughly with absolute ethanol and dried under vacuum. Yield ~ 90%; m.p. 165 °C; ^{1}H NMR: δ 2.83 (s, 4H), 3.06 (s, 12H), 6.69–6.62 (m, 4H), 7.11–7.07 (m, 4H), 7.31–7.28 (m, 4H), 7.73–7.71 (m, 4H), 9.72 (s, 2H); ES-MS (*m*/*z*): 537(20%) $[M-H]^+$. Anal. Calc. for $C_{32}H_{34}N_4S_2$: C, 71.34; H, 6.36; N, 10.40. Found: C, 71.42; H, 6.45; N, 10.49%.

2.3. Methods

The ligand **L** was characterized by elemental analysis, ^{1}H NMR and ESI-MS spectra. ^{1}H NMR spectra were recorded on a JEOL JNM-LA400 FT (400 MHz) instrument in $CDCl_3$ with Me_4Si as the internal standard. UV–Vis spectra were recorded on a JASCO V-570 spectrophotometer in CH_3CN at 298 K. Fluorescence spectra in solution phase were recorded on a Perkin Elmer LS50B, luminescence spectrometer at 298 K. Melting points were determined with an electrical melting point apparatus by PERFIT, India and were uncorrected. The electrospray mass spectra (ES-MS) were recorded on a MICROMASS QUATTRO Quadruple Mass Spectrometer. Each sample dissolved in acetonitrile and introduced into the ESI source through a syringe pump at the rate of 5 μl/min. The ESI capillary was set at 3.5 kV and the cone voltage was 40 V. The spectra were collected in 6 s scans and the printouts were averaged of 6–8 scans. Microanalyses for the complexes were obtained from CDRI, Lucknow, India.

Fluorescence quantum yields of all the compounds were determined by comparing the corrected spectrum with that of quinine sulfate ($\phi_F = 0.54$) in 1 N sulfuric acid [15], $\lambda_{ex} = 350$ nm, taking the area under the total emission.

2.3.1. Measurement of two photon absorption cross-section (δ)

Two-photon absorption cross-section values are measured by open aperture Z-scan technique [16]. The femtosecond experimental scheme involves mode-locked Coherent Mira titanium: sapphire laser (Model 900) which is pumped by Coherent Verdi frequency doubled Nd:vanadate laser. The model 900 Mira is tunable from 740 to 900 nm and its repetition rate is 76 MHz. The duration of the pulse is 150 fs as measured by autocorrelation technique. We used 880 nm wavelength here for all the measurements. Using a 20 cm focal length lens, the beam is

focused into a 1 cm long cell filled with sample, where it easily produces GW-level intensity at the focal point of the lens. The sample is scanned through the focal point using a motorized translation stage (model ESP 300), which can step with a minimum resolution of 0.1 μm. This allows a smooth intensity scan for the samples in this wavelength. The transmitted beam, after passing through the sample is focused into the aperture of a UV-enhanced amplified silicon photo detector (Thorlabs DET 210) by using a 7.5 cm focal length lens. The signal is measured in an oscilloscope (Tektronix TDS 224), which is finally interfaced with the computer using GPIB card (National Instruments). The data are acquired using LabVIEW programming. The nonlinear absorption coefficient β is obtained [17], by fitting our measured transmittance values to the following formula:

$$T(z) = 1 - \beta I_0 L/(2(1 + z^2/z_0^2)),$$

where β = nonlinear absorption coefficient, I_0 = on-axis electric field intensity at the focal point in absence of the sample, L = sample thickness, z_0 = Rayleigh range = $\pi w_0^2/\lambda$, w_0 is the minimum spot size at the focal point. The β values are obtained by curve fitting the measured open-aperture traces with the above equation. After getting the value of β, the TPA cross-section δ in GM unit of one solute molecule is given by the following expression:

$$\delta = \beta h v/N \cdot c \cdot 10^{-3},$$

where v is the frequency of the incident laser beam, N is Avogadro constant, c is the concentration of the compound in 90:10 (v/v) mixture of DCM and CH_3CN solvent. Rhodamine 6G is taken as the reference to calibrate the measurement technique for which the δ value is known in the literature [18].

2.3.2. Binding constant determination

The binding constants (K_s) for the complexes between **L** and metal ions were determined by UV–Vis spectroscopic titration of dilute solution of **L** against metal ion solution in 90:10 (v/v) mixture of DCM and CH_3CN solvent. The concentration of metal ions was in the range 1×10^{-5}–1×10^{-3}M. The ligand concentration was 1×10^{-5} M. The linear fit of the absorption spectral data at a particular wavelength for 1:1 complexation was obtained by applying the following equation [19]

$$A_0/(A - A_0) = [a/(b - a)][(1/K_s[\mathrm{M}]) + 1],$$

where A_0 and A are the absorbance of the metal-free ligand and the ML complex, respectively and [M] is the concentration of various metal ions added for complexation. When $A_0/(A - A_0)$ is plotted against the metal ion concentration $[\mathrm{M}]^{-1}$, K_s is directly obtained from the intercept/slop ratio. The details of the theoretical analysis of the stoichiometries and corresponding binding constant determination are available [20] in the literature. Here the reported values are consistent with good correlation coefficients ($\geqslant 0.98$).

3. Results and discussion

In ligand **L**, two imine moieties along with two sulfur groups (N_2S_2 unit) form a 3-D cavity with moderately large residual electron density capable of binding metal ions (Scheme 1). This makes **L** an attractive candidate for modulation of TPA property through metal ion recognition events.

3.1. UV–Vis absorption spectroscopy and binding constant determination in metal complexes

Compound **L** is highly soluble in DCM but sparingly soluble in CH_3CN solvent. Thus, all the photophysical properties of **L** were studied in mixed DCM/CH_3CN solvents. It exhibits a broad absorption band at $\lambda_{max} = 358$ nm in 90:10 (v/v) mixture of DCM and CH_3CN solution with $\varepsilon_{max} = 7.5 \times 10^4$ mol L^{-1} cm^{-1} (Table 1), which is attributable [21] to the combined locally excited (LE) and intraligand charge transfer (ILCT) from the dimethylamine moiety to the imine moiety. Upon addition of metal ions, two well-resolved broad peaks appear where the λ_{max} of higher energy band is located in the range of 337–355 nm and the lower energy band is located at $\lambda_{max} = 450$ nm. The ε_{max} values are highly sensitive to the metal ion inputs. Upon complexation, there is a considerable change in the ε_{max} value of the lower energy band in case of Zn(II) and Mg(II) ion input compare to Ca(II) and Cd(II) ion input. The reverse situation appears in case of the higher energy band (Table 1). To explain this phenomenon, the complex stability constant values ($\log K_s$) are calculated with 1:1 metal–ligand ratio as confirmed by the isobestic point obtained at 400 nm (Fig. 1). For the complexation of **L** with Zn(II) and Mg(II), the $\log K_s$ values are found to be 4.6 and 4.4 respectively, whereas the $\log K_s$ values for Cd(II) and Ca(II) are 3.6 and 3.4, respectively. Based on the stability constant data, it is

Table 1
Liner and nonlinear spectroscopic data for **L**

Compound	λ_{abs}/nm ($\varepsilon \times 10^4$/mol L^{-1} cm^{-1})	$\lambda_{max\text{-}em}$ (nm)	δ (GM)	$\log K_s$	$\phi \times 10^{-3}$	$\Delta\delta$ (%)
L	358 (7.5)	422	2300		0.44	
L–Zn^{2+}	338 (4.4), 450 (7.6)	384	1580	4.6	12.8	31
L–Cd^{2+}	347 (5.9), 463 (0.6)	409	1960	3.6	4.2	14
L–Mg^{2+}	338 (5.2), 450 (5.1)	386	1650	4.4	10.2	28
L–Ca^{2+}	355 (6.7), 465 (0.7)	407	1930	3.4	2.7	16

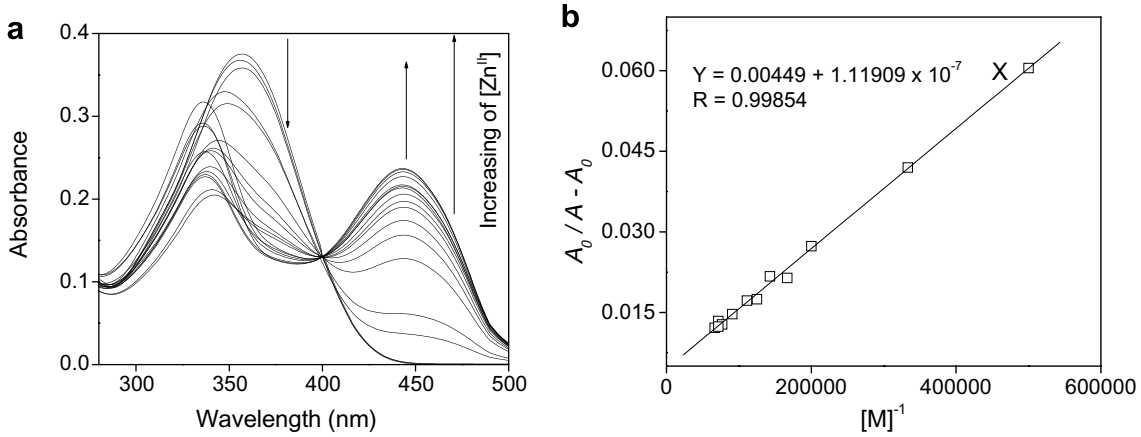

Fig. 1. (a) UV–Vis spectra of **L** upon addition of Zn(II) ion. (b) Linear regression plot of $A_0/(A - A_0)$ as a function of inverse concentration of Zn(II) ion added to **L**.

speculated that due to small size both Zn(II) and Mg(II) ions can easily fit into the cavity of **L** and localize the electrons of the imine moieties to greater extent compared to Ca(II) and Cd(II) ions which, in turn, becomes a strong acceptor. As a result, Zn(II) and Mg(II) ions induce more asymmetric D–π–A character to **L** in compare to Ca(II) and Cd(II) ions.

3.2. Emission studies

Compound **L** shows very low broad emission in a mixture of DCM and CH_3CN solvent. The quantum yield ($\phi_F = 0.00044$) is very low due to weak ICT from the terminal dimethylamino to the imine (referenced to quinine sulfate [15] in 1 N sulfuric acid, $\lambda_{ex} = 350$ nm, $\phi_F = 0.54$). In presence of metal ions, **L** exhibits enhanced fluorescence intensity with two well-resolved peaks assignable to the locally excited (LE) transition and the intramolecular charge transfer (ICT) transition from the donor dimethylamino to the metal bound imine moieties, respectively (Fig. 2) [22]. In case of Zn(II) and Mg(II) ions, the fluorescence quantum yield increases up to ~25 times compared to the metal-ion free receptor **L** (Table 1). The isomerization of the imine bond in the excited state prevail the fluorescence property of the free ligand [23]. However, in presence of metal ion the isomerization of the imine bond is restricted due to the formation of metal–nitrogen bond, which reflects the increment of quantum yield of the metal–ligand complex.

3.3. Nonlinear optical properties

The TPA cross-section (δ) value of **L** was measured in 90:10 (v/v) mixture of DCM/CH_3CN solvent in absence and presence of metal ions at 880 nm. The Z-scan traces are shown in Fig. 3 while the δ values for free and complexed **L** are given in Table 1. The high δ value of 2300 GM for **L** can be attributed to the presence of two D–π–π′–π–D chromophoric units with extended conjugation through the two aromatic rings for each unit. Several reports are available in the literature [24] showing increment of the δ values to different extents with the increase of the chromophore number density.

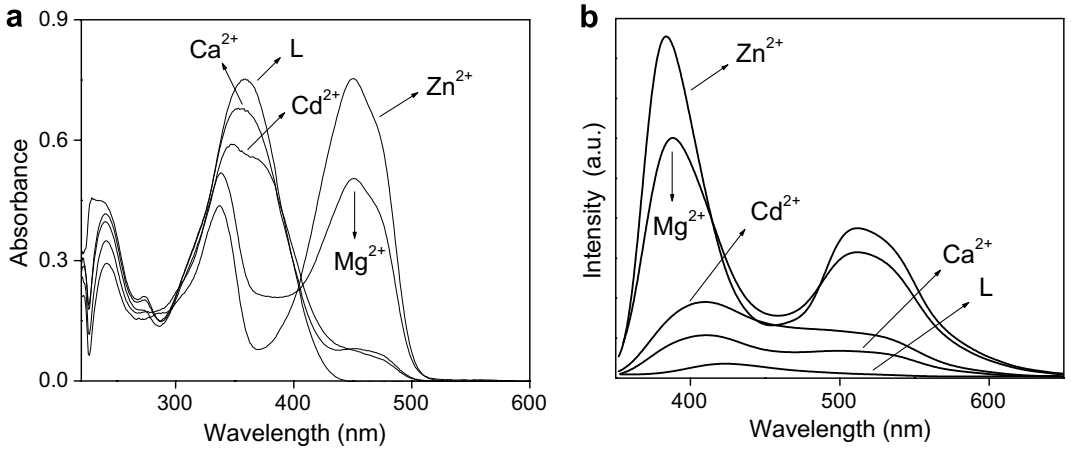

Fig. 2. (a) UV–Vis spectra of **L** alone and in presence of different metal ion inputs in 90:10 (v/v) mixture of DCM/CH_3CN (1×10^{-5} M). (b) Emission spectra of **L** alone and in presence of Zn(II), Cd(II), Mg(II) and Ca(II) in 90:10 (v/v) mixture of DCM/CH_3CN (1×10^{-5} M).

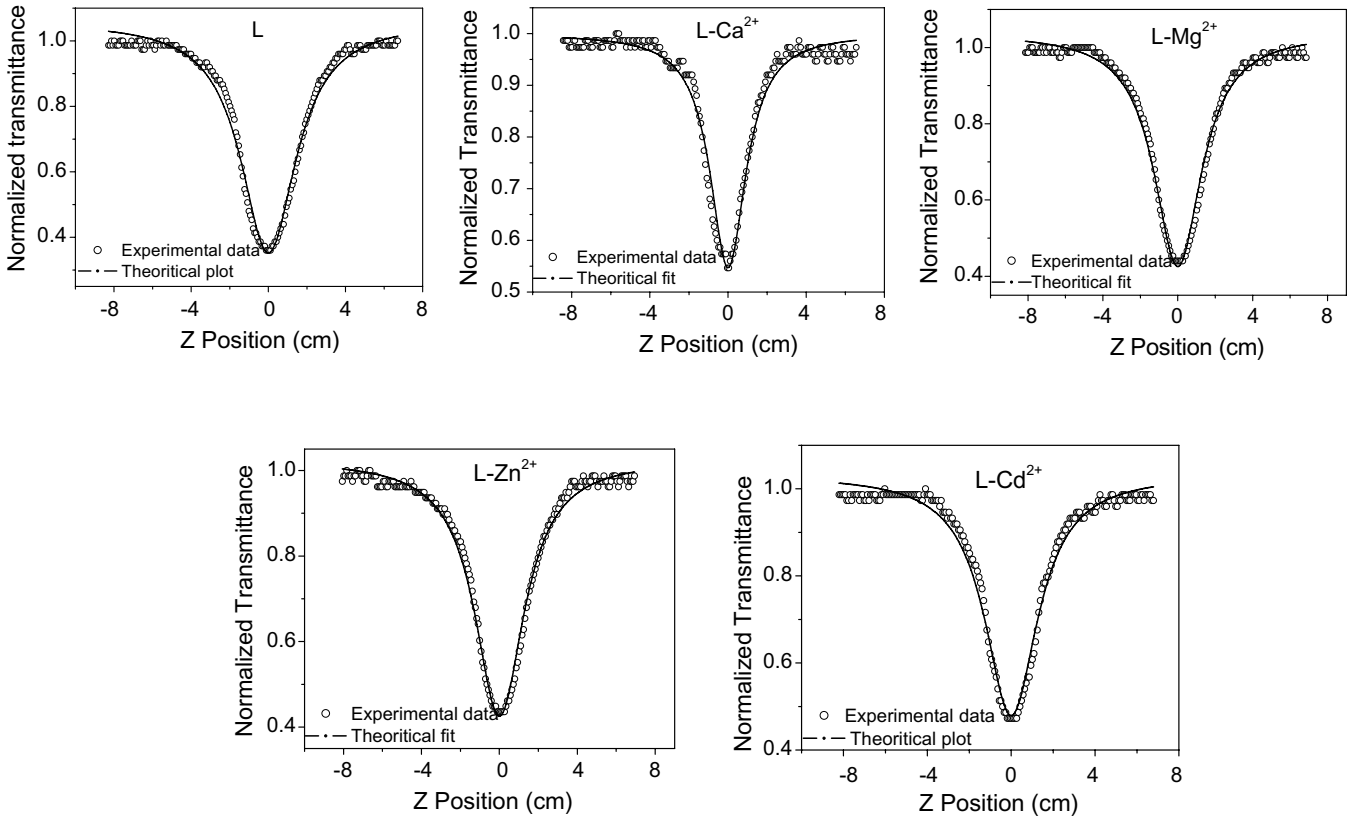

Fig. 3. Open-aperture Z-scan traces of **L** (conc. 5×10^{-4} M) and in presence of Ca(II), Mg(II), Zn(II) and Cd(II) ions input. Solid lines are the best fitted of the experimental data.

When a metal ion is added to **L**, it binds at the N_2S_2 donor site as shown in Scheme 1. The metal coordination induces considerable localization of the electrons causing lowering of the δ values compared to the metal-free **L**. Both Zn(II) and Mg(II) ions decrease the TPA cross-sectional value more in comparison to Ca(II) and Cd(II) consistent with higher binding constant values for the former two ions making the molecular charge transfer character of **L** more asymmetric in nature.

3.4. Theoretical studies

The molecular geometries of the ligand and its Zn(II) complex were optimized at the B3LYP/6-31G* level in the density functional theory (DFT) formalism by using the GAUSSIAN 03 program package [25] to study the effect of the nature of ligand in the metal complex on two photon absorption properties. The geometries corresponding to global minima obtained with the semi-empirical AM1 method (gradient <0.001, Hyperchem version 7.0; Hypercube Inc.) were similar to the DFT results for all the cases. The transition energies of the compounds were then calculated by using time-dependent DFT (TD-DFT) method using the same functional (B3LYP) with the same basis set (6-31G*). The design of the pushing donor groups allows assessing the effect of donor strengths. To gain better insight into the effects of Zn^{+2} on the two-photon properties of the chromophores, quantum chemical calculations were performed for three different models of the ligand as well as three different metal–ligand complex models excluding the anions for simplicity. The model compounds are based upon *cis*/*trans* isomerism of imine bonds and the models are *trans–trans*, *trans–cis* and *cis–cis* geometry along the two strands of the ligand.

The global energy-minimized geometry is obtained for the *trans–trans* orientation of the imine bonds for the ligand (Fig. 4). But in case of metal complex the nature of two imine bonds become different and the lowest energy structure is obtained for *trans–cis* orientation. This change in geometry results in lower TPA values for the metal–ligand complex. The *trans–trans* geometry in the ligand is more favorable than the other two models mainly due to less steric hindrance between the π-arms of the ligand; hence π conjugation is quite effective through the chromophoric length of the ligand. Any one of the model complexes for ligand does not provide a favorable molecular geometry for metal complexation as the N(1)–N(2) distances are more than 9 Å i.e., too long to bind a metal ion. As a result, the geometry of the ligand is severely modified via rotation of the central C–C bond between two sulfur atoms. The Zn–S bond distance is the guiding factor in stabilization of this particular geometry over the other two models. In all the cases, the sulfur atoms in the ligand play the role of weak coordinating atoms to bind with metal. The calculated Zn–S bond

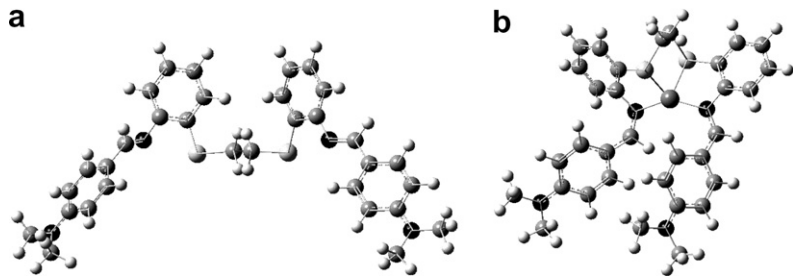

Fig. 4. The global energy-minimized geometry of (a) the ligand and (b) its Zn(II) complex.

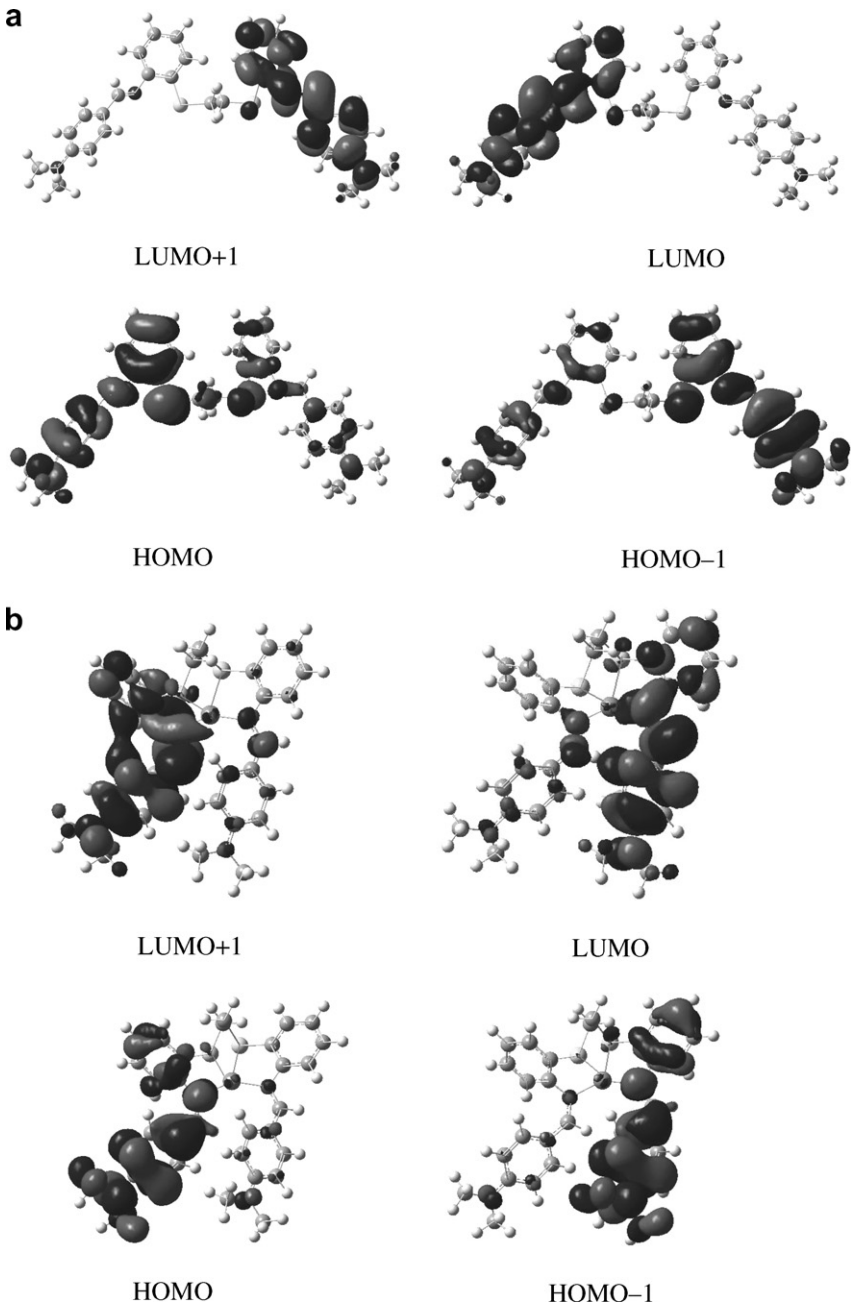

Fig. 5. Contour surfaces of HOMO−1, HOMO, LUMO and LUMO+1 for (a) the ligand and (b) its Zn(II) complex.

distances (2.45 Å) are similar to the values reported for other Zn(II) complexes with thioether ligands [26]. In the present case, metal–sulfur interaction snaps the conjugation of the π electron cloud that was present throughout the side arms in the free ligand (Fig. 5). This reduces charge transfer and in turn reduces the two-photon absorption cross-

section. In some case, this decrease of the transition dipole moment can be explained by analyzing the transition nature of the higher-lying (TPA target) excited state as well as the lower-lying (intermediate) state. There is a delocalization of π electron from the donor dimethylamino group to the nitrogen atom of imine bond. The planar geometry in the two arms (torsion angle between dimethylamino group and imine group is less than 1°) in the favorable geometry of the ligand is distorted to a greater extent when complexed with Zn(II) (torsion angle is grater than 14°). These distortions from planarity lead to diminished conjugation and in turn to low TPA cross-section in the complex. The summation of the angle around the imine nitrogen atom after complexation suggests sp^2 geometry of the nitrogen in the metal-bound state. This is consistent with the imine nitrogen atoms being strongly, but not completely, decoupled from the π system when Zn^{+2} ion is complexed by the ligand.

Comparing the energy level diagrams of the ligand and its complex with Zn(II) ion, it is found that complexation decreases the HOMO–LUMO energy gap. This is corroborated by single photon absorption spectra that show red shift upon metal complexation. Table 2 summarizes the calculated one-photon absorption (OPA) properties (the maximum OPA wavelengths λ_{max}, transition natures and oscillator strengths f) of studied molecules and the available experimental values. As shown in Table 2, our calculated results deviate slightly from the experimental values. This is understandable, because the experimental values were measured in the polar solvent and were affected by the counter ions in solution, while our calculations were carried out in vacuum. Upon coordination, the acceptor strength of the imine moiety is enhanced, resulting in a red shift of the maximum OPA wavelength.

Generally the frontier molecular orbitals, especially HOMO−1, HOMO, LUMO and LUMO+1, have important contributions to electronic transition during two-photon excitation. In Fig. 5, the contours of the non-degenerate HOMO−1, HOMO, LUMO and LUMO+1 for the ligand and its Zn complex are shown. In the case of free ligand HOMO−1 and LUMO+1 are mainly distributed in the same strand of the ligand while HOMO and LUMO are mainly positioned on the other strand. By close look at the contour diagrams we can say that the HOMO–LUMO transition is nothing but the $\pi \rightarrow \pi^*$ transition of the chromophore. In case of Zn complex, the HOMO−1 and LUMO are distributed in the strand where *trans* geometry is observed around the imine bond. Here, HOMO and LUMO+1 are mainly positioned in the *cis* imine based strand. Thus, the HOMO–LUMO transition can be said to be the reflection of intra-ligand charge transfer (ILCT). From the viewpoint of the HOMO of ligand as well as Zn complex it can be concluded that the π conjugation from one strand of the ligand to the other strand is sufficiently reduced in the metal complex. This is due to the involvement of π orbitals of the sulfur atoms in the ligand but this π cloud around the sulfur atoms are almost negligible in the Zn complex as it forms a weak σ bond with the metal.

Table 2
Theoretical OPA properties and transition dipole moments for studied compounds

Compound	**L**	**L**–Zn^{2+}
λ_{abs} (nm) (experiment)	358	450
λ_{max} (nm) (theoretical)	362, 354, 348	464
Transition nature	HOMO−2 → LUMO+1 HOMO−1 → LUMO+1 HOMO → LUMO+1 HOMO−1 → LUMO HOMO → LUMO	HOMO → LUMO
Oscillator strength (f)	0.2583, 0.0376	0.0025
E_{ge} (eV)	3.26	3.11
M_{ge} (D)	6.17	10.95
$M_{ee'}$ (D)	12.80	5.46
δ (GM)	2300	1580

The two-photon absorption properties of conjugated systems can be described by looking at the transition dipole moments [2]. For this, a simple model can be invoked containing three electronic states: the ground state (g), the lowest excited state (e), and a higher lying two-photon state (e′). The two-photon absorption cross-section depends on the transition dipole moments (M) between states g and e, and between states e and e′. After determining the transition moment M_{ge} for the g → e transition through TD-DFT method, and assuming $\Gamma_{ge'} \approx 0.1$ eV (a value consistent with the bandwidth of the two-photon spectra for many chromophores), the excited-state transition moment $M_{ee'}$ can be estimated, based on experimental data, via the available literature method [14]. In this context, the changes in the magnitude of two-photon absorption cross-section of the ligand on cation binding can be attributed to a moderate reduction of the excited-state transition dipole moment ($M_{ee'}$) from 12.80 to 5.46 D (Table 2) while M_{ge} is calculated to be almost opposite for the unbound and bound forms of the chromophore (6.17 and 10.95 D, respectively). These changes in the transitional dipole moment values reflect in the reducing δ value of the Zn complex.

4. Conclusion

In conclusion, we have reported the synthesis of a new ion responsive molecule in the format donor–acceptor–acceptor–donor that exhibits large TPA cross-section measured in femtosecond regime. Its TPA activity reduces in presence of selective metal ions to different extents in consistent with their stability constant values. In case of Zn(II) and Mg(II) ions, the δ value decreases, respectively, by 31% and 28%. Interestingly, this ligand shows enhancement of fluorescence upon metal binding where the quantum yield increases up to 25 times compared to metal-free **L**. Fluorophores with large two-photon absorption cross-section are potentially important in TPLSM applications. Theoretical calculations carried out at the B3LYP/6-31G* level in density functional theory (DFT) formalism show that upon metal binding, the π conjugation diminishes significantly as also the transition moment leading to lower TPA

cross-section in the metal complexes. Further studies on similar systems are in progress in our laboratory.

Acknowledgments

Financial support received from DRDO & DST, New Delhi, India (to P.K.B.) is gratefully acknowledged. D.G. thanks DST, MCIT (India) and international SRF program of Welcome Trust (UK) for the financial grant. K.K.S. thanks CSIR for SRF and A.N. thanks UGC for SRF.

Appendix A. Supplementary material

Characterization of the ligands **L**: ESI-MS, ^{1}H NMR, and Open-aperture Z-scan traces of reference Rhodamine 6G. Supplementary data associated with this article can be found, in the online version, at doi:10.1016/j.jorganchem.2007.07.013.

References

[1] (a) R.H. Kohler, J. Cao, W.R. Zipfel, W.W. Webb, M.R. Hansen, Science 276 (1997) 2039;
(b) J.D. Bhawalkar, G.S. He, P.N. Prasad, Opt. Commun. 119 (1995) 587;
(c) J.H. Strickler, W.W. Webb, Adv. Mater. 5 (1993) 479;
(d) Q. Zheng, G.S. He, T.-C. Lin, P.N. Prasad, J. Mater. Chem. 13 (2003) 2499;
(e) J.D. Bhawalkar, N.D. Kumar, C.F. Zhao, P.N. Prasad, J. Clin. Laser Med. Surg. 15 (1997) 201.
[2] M. Albota, D. Beljonne, J.-L. Bredas, J.E. Ehrlich, J.-Y. Fu, A.A. Heikal, S.E. Hess, T. Kogej, M.D. Levin, S.R. Marder, D. McCord-Maughon, J.W. Perry, H. Röckel, M. Rumi, G. Subramaniam, W.W. Webb, X.-L. Wu, C. Xu, Science 281 (1998) 1653.
[3] (a) W.J. Yang, D.Y. Kim, M.-Y. Jeong, H.M. Kim, Y.K. Lee, X. Fang, S.-J. Jeon, B.R. Cho, Chem. Eur. J. 11 (2005) 4191;
(b) S.J. Chung, K.-S. Kim, T.H. Lin, G.S. He, J. Swiatkiewicz, P.N. Prasad, J. Phys. Chem. B 103 (1999) 10741;
(c) J. Yoo, S.K. Yang, M.-Y. Jeong, H.C. Ahn, S.-J. Jeon, B.R. Cho, Org. Lett. 5 (2003) 645;
(d) L. Antonov, K. Kamada, K. Ohta, F.S. Kamounah, Phys. Chem. Chem. Phys. 5 (2003) 1193.
[4] K.D. Belfield, K.J. Schafer, W. Mourad, B.A. Reinhardt, J. Org. Chem. 65 (2000) 4475.
[5] O. Mongin, L. Porres, L. Moreaux, J. Mertz, M. Blanchard-Desce, Org. Lett. 4 (2002) 719.
[6] W.H. Lee, H. Lee, J.A. Kim, J.-H. Choi, M. Cho, S.-J. Jeon, B.R. Cho, J. Am. Chem. Soc. 123 (2001) 10658.
[7] M. Drobizhev, A. Karotki, A. Rebane, Opt. Lett. 26 (2001) 1081.
[8] (a) Q. Zheng, G.S. He, P.N. Prasad, J. Mater. Chem. 15 (2005) 579;
(b) S.K. Hurst, M.G. Humphrey, T. Isoshima, K. Wostyn, I. Asselberghs, K. Clays, A. Persoons, M. Samoc, B. Luther-Davices, Organometallics 21 (2002) 2024.
[9] S. Das, A. Nag, D. Goswami, P.K. Bharadwaj, J. Am. Chem. Soc. 128 (2006) 402.
[10] X.M. Wang, D. Wang, G.Y. Zhou, W.T. Yu, Y.F. Zhou, Q. Fang, M.H. Jiang, J. Mater. Chem. 11 (2001) 1600.
[11] L. Frediani, Z. Rinkevicius, H. Ågren, J. Chem. Phys. 122 (2005) 244104.
[12] (a) Y. Suzuki, H. Komatsu, T. Ikeda, N. Saito, S. Araki, D. Citterio, H. Hisamoto, Y. Kitamura, T. Kubota, J. Nakagawa, K. Oka, K. Suzuki, Anal. Chem. 74 (2002) 1423;
(b) A. Takahashi, P. Camacho, J.D. Lechleiter, B. Herman, Physiol. Rev. 79 (1999) 1089.
[13] (a) C. Xu, R.M. Williams, W. Zipfel, W.W. Webb, Bioimaging 4 (1996) 198;
(b) C. Xu, W.W. Webb, J. Opt. Soc. Am. B 13 (1996) 481.
[14] S.J.K. Pond, O. Tsutsumi, M. Rumi, O. Kwon, E. Zojer, J.L. Bredas, S.R. Marder, J.W. Perry, J. Am. Chem. Soc. 126 (2004) 9291.
[15] S.R. Meech, D. Phillips, J. Photochem. 23 (1983) 193.
[16] M. Sheik-Bahaei, A.A. Said, T. Wei, D.J. Hagan, E.W. Van Stryland, IEEE J. Quantum Electron. 26 (1990) 760.
[17] (a) D. Kim, A. Osuka, M. Shigeiwa, J. Chem. Phys. A 109 (2005) 2996;
(b) H. Rath, J. Sankar, V. Prabhuraja, T.K. Chandrasekhar, A. Nag, D. Goswami, J. Am. Chem. Soc. 127 (2005) 11608.
[18] P. Sengupta, J. Balaji, S. Banerjee, R. Philip, G. Ravindra Kumar, S. Maiti, J. Chem. Phys. 112 (2000) 9201.
[19] (a) J. Bourson, J. Pouget, B. Valeur, J. Phys. Chem. 97 (1993) 4552;
(b) S. Banthia, A. Samanta, J. Phys. Chem. B 106 (2002) 5572.
[20] S. Fery-Forgues, M.T. Le Bries, J.P. Guetté, B. Valeur, J. Phys. Chem. 92 (1988) 6233.
[21] P.R. Bangal, S. Chakravorti, J. Photochem. Photobiol. A 116 (1998) 191.
[22] (a) C.H. Zhang, Z.B. Chen, Y.B. Jiang, Spectrochim. Acta A 60 (2004) 2729;
(b) W. Rettig, Angew. Chem., Int. Ed. Engl. 25 (1986) 971.
[23] J.-S. Wu, W.-M. Liu, X.-Q. Zhuang, F. Wang, P.-F. Wang, S.L. Tao, X.H. Zhang, S.K. Wu, S.T. Lee, Org. Lett. 9 (2007) 33.
[24] (a) S.J. Chung, K.-S. Kim, T.H. Lin, G.S. He, J. Swiatkiewicz, P.N. Prasad, J. Phys. Chem. B 103 (1999) 10741;
(b) J. Yoo, S.K. Yang, M.Y. Jeong, H.C. Ahn, S.J. Jeon, B.R. Cho, Org. Lett. 5 (2003) 645.
[25] M.J. Frish et al., Gaussian 03 Program (Revision C. 02), Gaussian Inc., Wallingford, CT, 2004.
[26] (a) B. Kersting, Angew. Chem. Int. Ed. 40 (2001) 3987;
(b) D.C. Haagenson, D.F. Moser, L. Stahl, Inorg. Chem. 41 (2002) 1245.